Strong Quantum Coherence between Fermi Liquid Mahan Excitons

J. Paul,[1] C. E. Stevens,[1] C. Liu,[1] P. Dey,[1] C. McIntyre,[1] V. Turkowski,[2] J. L. Reno,[3] D. J. Hilton,[4] and D. Karaiskaj[1,*]
[1]Department of Physics, University of South Florida, 4202 East Fowler Avenue, Tampa, Florida 33620, USA
[2]Department of Physics, University of Central Florida, Orlando, Florida 32816, USA
[3]CINT, Sandia National Laboratories, Albuquerque, New Mexico 87185, USA
[4]Department of Physics, University of Alabama at Birmingham, Birmingham, Alabama 35294, USA
(Received 6 August 2015; revised manuscript received 11 March 2016; published 14 April 2016)

In modulation doped quantum wells, the excitons are formed as a result of the interactions of the charged holes with the electrons at the Fermi edge in the conduction band, leading to the so-called "Mahan excitons." The binding energy of Mahan excitons is expected to be greatly reduced and any quantum coherence destroyed as a result of the screening and electron-electron interactions. Surprisingly, we observe strong quantum coherence between the heavy hole and light hole excitons. Such correlations are revealed by the dominating cross-diagonal peaks in both one-quantum and two-quantum two-dimensional Fourier transform spectra. Theoretical simulations based on the optical Bloch equations where many-body effects are included phenomenologically reproduce well the experimental spectra. Time-dependent density functional theory calculations provide insight into the underlying physics and attribute the observed strong quantum coherence to a significantly reduced screening length and collective excitations of the many-electron system.

DOI: 10.1103/PhysRevLett.116.157401

Optical excitations in semiconductors lead to the formation of Coulomb bound electron-hole pairs known as excitons. The excitons in GaAs quantum wells to first order are well explained by the Wannier theory with binding energies that vary with the quantum well thickness [1]. As a result of the lowering of the symmetry in the growth direction of the quantum well structure, the orbital degeneracy at the top of the valence band is lifted leading to heavy (HH) and light hole (LH) excitons. The quantum coherence between Wannier excitons in undoped semiconductor quantum wells has been studied extensively using time-integrated, time-resolved, and spectrally resolved four-wave mixing (FWM) spectroscopy. These studies have provided important insight into the many-body interactions taking place [2–4]. Quantum coherence between the heavy and light hole excitons was first observed as quantum beating in the FWM decay. However, one-dimensional FWM spectroscopy could not unambiguously distinguish between quantum and polarization beating. It is the advent of two-dimensional Fourier transform (2DFT) spectroscopy that could differentiate between the two processes [5].

As the quantum wells are doped, the Coulomb interactions are screened and the many-body interactions are altered. At low doping concentration, the spectra are dominated by excitonic effects, and at moderate dopings, charged excitons or trions can form. Recently, an unexpected coherent coupling between exciton and trions in CdTe/CdMgTe quantum wells was observed [6]. This was rather surprising despite the rather weak effect, since the screening provided by the charged carriers was thought to destroy any coherent coupling. With increasing doping, excitons are thought to quickly lose their identity and eventually unbind, while the spectral weight moves toward the Fermi level. The spectra start to display a broadened singularity at the Fermi level leading to an energy shift between the photoluminescence and absorption spectra. Although the bound excitonic state is no longer stable, in the "rigid Fermi sea" picture a bound state with respect to the Fermi level still exists. This state was first discussed by Mahan in highly doped bulk semiconductors and metals and is referred to in the literature as the "Mahan exciton" [7,8].

The optical excitations not only introduce new electrons in the conduction band that interact with the other electrons, but also introduce positive charges in the valence band that interact with the Fermi liquid. Upon optical excitation from the HH and LH valence bands, the electrons should quickly lose their identity [Fig 1(a)], where now bound states are formed between the positively charged holes and the collective excitation of the Fermi edge. Therefore, the binding energy of Mahan excitons can be regarded as a shift of the energy of the collective electron state due to the positive potential of the hole. As a result of the collective nature of the Mahan exciton, any quantum coherence or memory effects should be quickly extinguished.

Surprisingly, in the present study strong quantum coherence is observed that is quantitatively stronger than observed in undoped quantum wells between HH and LH Wannier excitons [5]. This quantum coherence manifests itself in cross peaks in the 2DFT spectra that are stronger than observed in undoped quantum wells. The

intensities of the cross peaks in the 2DFT spectra relative to diagonal peaks depend on the polarizations of the excitation pulses. As a result, certain polarizations can enhance two-quantum contributions to the 2DFT spectra and lead to stronger cross peaks. The one-quantum S_I 2DFT spectra of Mahan excitons show stronger cross peaks using circularly polarized excitation pulses. It should be pointed out here that we refer to quantum coherence as a coupling of the excitons via a common state, which should be distinguished from polarization interference originating from independent states [11]. Moreover, the S_{III} 2DFT spectra originate solely from two-quantum contributions to the nonlinear optical response [12]. Therefore, cross peaks observed in the S_{III} spectra unambiguously confirm the nature of the cross peaks in our 2DFT spectra of Mahan excitons, which originate from quantum coherent coupling and not from polarization interference [6].

Furthermore, the observed line shapes of the cross peaks in the S_I spectra extend energetically above the LH excitonic resonance, which indicate contributions from virtual "continuum states" above the Fermi level. Such collective excitations above the Fermi energy are a clear demonstration of the many-body nature of the Mahan exciton and are modeled here by a series of closely spaced resonances above the LH energy that dephase very rapidly [13,14]. The experimental 2DFT spectra are qualitatively well reproduced using the optical Bloch equations, where the many-body effects such as excitation induced dephasing (EID) and excitation induced shift (EIS) are included phenomenologically.

However, in order to gain deeper understanding into the unexpected quantum coherence between the HH and LH Mahan excitons, we performed time-dependent density functional theory (TDDFT) calculations [15]. The TDDFT calculations confirm the existence of bound states for both the HH and LH Mahan excitons at this doping level with a binding energy that remains unchanged over a large range of doping concentrations. The occurrence of the quantum coherence between the HH and LH excitons was attributed to the reduced screening length in the quantum well. However, while the reduced screening explains why the quantum coherence is preserved, it does not explain the fact that it is enhanced when compared to the undoped quantum well excitons. We conclude that it is a result of collective excitation of the many-electron system that preserves or even enhances the quantum coherence, in analogy to strongly correlated electron systems.

Our present data demonstrate that the two-dimensional electron gas in modulation doped semiconductors forms an interesting system for quantitatively investigating many-body interactions [16,17]. Furthermore, in a strong magnetic field, the two-dimensional electrons form a correlated system that exhibits unique electronic transport properties such as the integer and fractional quantum Hall effect [18], which are also the subject of renewed interest as a result of the discovery of three-dimensional topological insulators [19]. Early light scattering and photoluminescence experiments in the quantum Hall regime have provided important insights into the physics of optical excitations at high magnetic fields [20–34]. The time-resolved coherent spectroscopy has also revealed one dramatic signature of many-body interactions, namely the enhancement of the signal for "negative delay τ" with increasing magnetic fields in a two-pulse FWM experiment [16,35,36].

The experimental setup used in the present study is shown in Fig. 1(b). Three laser pulses are incident on the sample and are separated by the time delays τ and T. By varying the "positive" time delay τ and monitoring the FWM intensity, referred to as time-integrated FWM, the dephasing time of excitons can be measured [Fig. 1(c)]. When the phase conjugate pulse A^* arrives at the sample last, the "negative" time delay leads to two-quantum coherences [Fig. 1(d)]. In order to generate the 2DFT spectra, a Fourier transform is performed with respect to two time variables, while the third is held constant. For "positive" delay τ the Fourier transform leads to 2DFT spectra in frequency domain described by $S_I(\omega_\tau, T, \omega_t)$ [Fig. 1(c)], whereas for negative delay τ two-quantum coherences appear in the $S_{III}(\tau, \omega_T, \omega_t)$ spectra [Fig. 1(d)] [37]. The advantages of multidimensional spectroscopy are well documented in the literature [38–41], where in semiconductor nanomaterials, 2DFT spectroscopy has provided insights into the microscopic details of the many-body interactions [12,42–46].

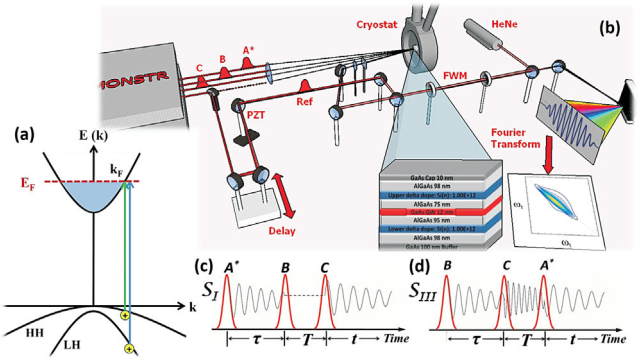

FIG. 1. (a) Schematic of the band structure. Electrons are excited from the HH and LH valence bands into the partially filled conduction band, leaving positively charged holes behind. (b) The four phase stabilized linearly polarized beams obtained from the MONSTR instrument described in Refs. [9,10] are focused on the sample, which is held in the cryostat at 5 K. The sample is mounted at a small angle with respect to the growth direction or normal the the sample surface, in order to allow for the FWM signal to be collected in reflection geometry. The FWM signal is heterodyned with a portion of the laser light (Ref) and dispersed in the spectrometer. The spectral interferograms are Fourier transformed leading to the 2DFT spectra. (c) The sequence of the laser pulses used in the S_I experiments, where A^* corresponds to the phase conjugate pulse. (d) The sequence of the laser pulses used in the S_{III} experiments (sample ID: VA0605).

The 2DFT measurements were performed on a modulation doped GaAs/AlGaAs single quantum well with 12 nm thickness and in-well carrier concentration of $\sim 4 \times 10^{11}$ cm^{-2}. The carrier concentration and the formation of Mahan excitons in the present sample have been confirmed by photoluminescence and time-integrated FWM (see Supplemental Material [47]) [48,49]. At this doping level, the nonlinear optical properties are dominated by the dynamical properties of the Fermi edge singularity or Mahan exciton. The experimental S_I 2DFT spectra are shown in Fig. 2 at four different polarizations, namely, $(HHHH)$, $(HVVH)$, $(\sigma^+\sigma^+\sigma^+\sigma^+)$, and $(\sigma^+\sigma^-\sigma^-\sigma^+)$, where the polarizations correspond to laser excitations A^*, B, C, and detection, respectively. The nonlinear optical processes described by the density matrix in the optical Bloch equations can be tracked much more conveniently using double-sided Feynman diagrams in Liouville space. Each polarization sequence selects specific pathways in Liouville space and potentially reduces the number of the double-sided Feynman diagrams that contribute to the nonlinear optical response [50–52]. As a result, select polarizations can change the intensity ratios between the diagonal and cross peaks. At $(HHHH)$ polarization the S_I 2DFT spectra are dominated by the HH exciton labeled as peak A, whereas the LH exciton is labeled as B. A strong cross peak C below the diagonal can also be observed. At $(HVVH)$ the only contribution allowed falls on the diagonal and the cross peaks are suppressed. Therefore, only the HH exciton on the diagonal (peak A) is observed. The LH exciton peak B should also be observed, but it is likely very weak as a result of the excitation laser being centered energetically toward the HH exciton.

Most importantly, at $(\sigma^+\sigma^+\sigma^+\sigma^+)$ and $(\sigma^+\sigma^-\sigma^-\sigma^+)$ two very strong cross peaks below the diagonal labeled C and above the diagonal labeled D are observed, which dominate the 2DFT spectra. At these polarizations, double-sided Feynman diagrams that contribute to the nonlinear 2DFT signal and involve two-quantum excitations are more dominant. Therefore, the cross peaks are stronger and are indicative of quantum coherence coupling via a common state. However, impure polarizations could potentially allow unwanted contributions to the S_I 2DFT spectra. Therefore, we further investigate the S_{III} 2DFT spectra which originate purely from two-quantum contributions. The appearance of cross peaks above and below the diagonal in the S_{III} 2DFT spectra in this case would confirm the quantum coherence.

The S_{III} 2DFT data at $(\sigma^+\sigma^+\sigma^+\sigma^+)$ are shown in Fig. 3 (left). Because of the fact that the S_{III} 2DFT spectra are based on the negative delay signal, they are rather weak. However, in addition to the two-exciton diagonal peaks A and B, two cross peaks can be observed. The cross peaks are enclosed in the white circles for clarity and are labeled as C and D. It should be pointed out here that the ω_T axis corresponds to $2 \times \omega_\tau$ because the S_{III} 2DFT spectra originate from two-quantum transitions [12]. The experimental spectra are reproduced in Fig. 3 (right) using the optical Bloch equations applying the same parameters used to reproduce the S_I experimental spectra.

Furthermore, in order to gain deeper understanding into the physics behind the observed quantum coherence, we performed state-of-the-art theoretical calculations that go beyond the phenomenological approach using the optical Bloch equations. The 2DFT spectra can also be theoretically modeled within the density-matrix version of TDDFT [15,53–56]. In the density-matrix TDDFT approach, the time-dependent Kohn-Sham equation is solved using time-dependent Hartree and exchange-correlation potentials. TDDFT has recently been successfully applied to study

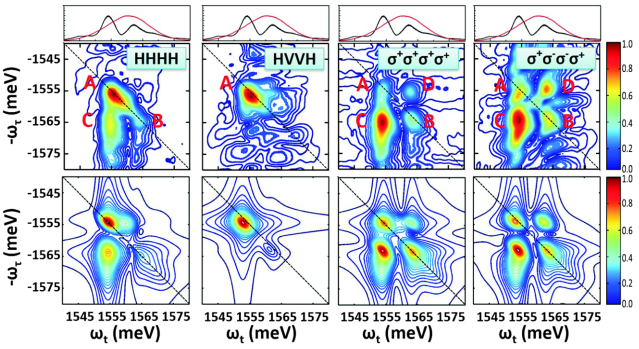

FIG. 2. Upper row: Experimental S_I 2DFT spectra at four different polarizations, namely, $(HHHH)$, $(HVVH)$, $(\sigma^+\sigma^+\sigma^+\sigma^+)$, and $(\sigma^+\sigma^-\sigma^-\sigma^+)$, where the polarizations correspond to A^*, B, C, and detection, respectively. The spectrally resolved FWM (black line) and the excitation laser spectrum (red line) are shown above the experimental spectra. Lower row: Theoretical spectra calculated using the optical Bloch equations where many-body effects such as EID and EIS are included phenomenologically.

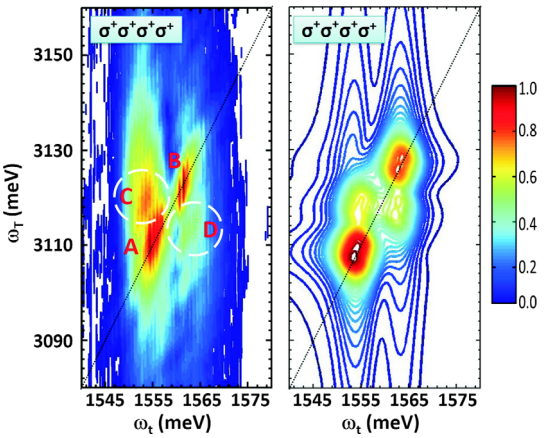

FIG. 3. Left: Experimental S_{III} 2DFT spectra at polarization $(\sigma^+\sigma^+\sigma^+\sigma^+)$, where the polarizations correspond to A^*, B, C, and detection, respectively. Right: Theoretical spectra calculated using the optical Bloch equations where many-body effects such as EID and EIS are included phenomenologically.

the excitonic effects in the frameworks of the time-dependent optimized effective potential approach [57,58]. This was achieved in combination with the Bethe-Salpeter equation [59,60] and by solving the TDDFT version of the semiconductor Bloch equations in the density-matrix representation [53,54]. Furthermore, the last approach was recently generalized to also include biexcitonic effects [55,56].

In order to calculate the S_I 2DFT spectra, we used the density-matrix TDDFT technique [55] with the screened Slater exchange-correlation kernel [56]. The TDDFT analysis was performed by using the static DFT Kohn-Sham wave functions and eigenenergies as input, which were obtained using the QUANTUM ESPRESSO package [61]. The corresponding S_I 2DFT spectra at $(HHHH)$ polarizations calculated using this approach are shown in Fig. 4 (left). Excellent agreement is found with the experimental data of Fig. 2, where not only both diagonal resonances A and B originating from the HH and LH excitons are reproduced, but also the strong cross peak C. We obtain further confirmation by calculating the binding energy of the HH, the LH excitons, and the HH-LH biexcitons as a function of doping. The results are shown in Fig. 4 (right) where at the doping levels studied here the Mahan excitons form a bound state with binding energies of ∼4.5, ∼1.0, and ∼0.9 meV for the HH exciton, LH exciton, and HH-LH biexciton, respectively. Even more surprising is that these quasiparticles continue to form bound states at even much higher doping levels and show very moderate decrease in binding energy with doping concentration.

The underlying physics leading to this effect is the reduced dielectric screening parameter due to the quantum confinement in the 12 nm quantum well. Despite a large number of additional scattering centers, namely electron dopants, the attractive potential between the electrons and holes remains strong even at rather high doping levels on the order of 10^{12}–10^{13} cm^{-2}. This can be simply demonstrated by estimating the Thomas-Fermi screening radius using the well-known relationship $r_{\mathrm{TF}} = \sqrt{\pi \varepsilon a_B / 4 k_F m}$,

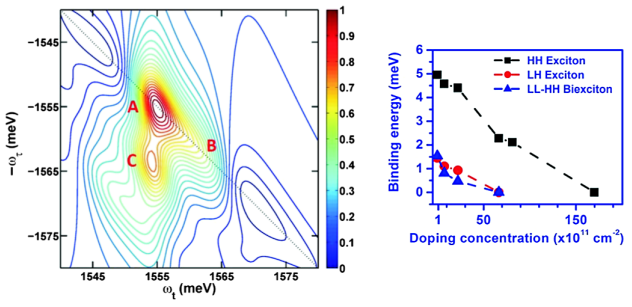

FIG. 4. Left: Calculated S_I 2DFT spectra at $(HHHH)$ polarizations using TDDFT. Right: Calculated binding energies for HH and LH excitons and HH-LH biexcitons as a function of doping using TDDFT.

which expressed in the relevant quantum well units leads to $r_{\mathrm{TF}} \approx 0.366\sqrt{\varepsilon/m}(l/N)^{1/6}$. Here, ε is the dielectric constant, m is the particle mass in units of m_0, l is the width of the well in nm, and N is the number of electrons per cm^{-2} divided by 10^{11}.

For a simple estimation of the Thomas-Fermi radius, we use $\varepsilon \sim 12.9$, the mass of the electron $m_e \approx 0.067$, the mass of the heavy hole $m_{\mathrm{HH}} \approx 0.45$, the mass of the light hole $m_{\mathrm{LH}} \approx 0.082$, the quantum well width $l = 12$ nm, and the number of electrons $N = 1$. We obtain for the electron $r^e_{\mathrm{TF}} \approx 7.6$ nm, heavy hole $r^{\mathrm{HH}}_{\mathrm{TF}} \approx 3.0$ nm, and light hole $r^{\mathrm{LH}}_{\mathrm{TF}} \approx 7.0$ nm. Although this estimation is rather simple, it demonstrates that the screening length is comparable to the quantum well width $l \sim 12$ nm. This indicates that the screening is greatly reduced as compared to the bulk case. Using this approach, we can estimate the increase in doping needed to reduce the binding energy by half. The number of electrons needs to increase by a factor of $2^6 = 64$, which corresponds to an increase from 10^{11} to 64×10^{11} cm^{-2}, which is nearly 2 orders of magnitude. This simple estimation is in excellent agreement with the TDDFT calculations shown in Fig. 4.

Finally, in order to gain insight into the dephasing mechanism as a function of doping density from the TDDFT calculations, we analyze the linear part of the exciton polarization function, described in detail in the Supplemental Material [47]. The dephasing time τ_d obtained was ∼1.3 ps for the excitons and ∼0.3 ps for biexcitons, well in agreement with recent experimental results [49]. Analyzing this equation can immediately reveal that the dephasing time τ_d is determined by a delicate balance between the screening parameter ε and the doping density. Initially, the increasing doping density leads to an increase in the dephasing time. This peculiar many-body effect is likely related to a collective coupling of many conduction electrons to a single hole. As expressed in the equations, with increasing doping, electron-electron scattering contributions become dominant and eventually lead to a decrease of τ_d.

In conclusion, we perform nonlinear optical 2DFT spectroscopy on a high mobility two-dimensional electron gas. Besides observing both the HH and LH Mahan exciton resonances along the diagonal of the 2DFT spectra, we also observe strong cross peaks above and below the diagonal, indicating quantum coherent coupling between the two resonances. The quantum coherence appears to be stronger than observed in undoped quantum wells between Wannier excitons. This is very surprising since the Mahan excitons occur as a result of the interaction of the positively charged holes with the ensemble of electrons in the conduction band. Therefore, screening and electron-electron interactions should destroy the quantum coherence. Instead, the reduced screening as a result of the quantum confinement in the quantum well combined with the collective nature of the electronic excitations at the Fermi edge enhance the

quantum coherence. The experimental results are in excellent agreement with detailed TDDFT calculations.

The work at USF and UAB was supported by the National Science Foundation under Grant No. DMR-1409473. The work at UCF was supported by the Department of Energy under Grant No. DE-FG02-07ER46354. This work was performed, in part, at the Center for Integrated Nanotechnologies, a U.S. Department of Energy, Office of Basic Energy Sciences user facility. Sandia National Laboratories is a multiprogram laboratory managed and operated by Sandia Corporation, a wholly owned subsidiary of Lockheed Martin Corporation, for the U.S. Department of Energy's National Nuclear Security Administration under Contract No. DE-AC04-94AL85000.

*karaiskaj@usf.edu

[1] G. H. Wannier, Phys. Rev. **52**, 191 (1937).
[2] H. Haug and S. W. Koch, *Quantum Theory of the Optical and Electronic Properties of Semiconductors* (World Scientific, Singapore, 2009).
[3] T. Meier, P. Thomas, and S. W. Koch, *Coherent Semiconductor Optics* (Springer, New York, 2007).
[4] J. Shah, *Ultrafast Spectroscopy of Semiconductors and Semiconductor Nanostructures* (Springer-Verlag, Berlin, 1999).
[5] X. Li, T. Zhang, C. N. Borca, and S. T. Cundiff, Phys. Rev. Lett. **96**, 057406 (2006).
[6] G. Moody, I. A. Akimov, H. Li, R. Singh, D. R. Yakovlev, G. Karczewski, M. Wiater, T. Wojtowicz, M. Bayer, and S. T. Cundiff, Phys. Rev. Lett. **112**, 097401 (2014).
[7] G. D. Mahan, Phys. Rev. **153**, 882 (1967).
[8] G. D. Mahan, Phys. Rev. **163**, 612 (1967).
[9] A. D. Bristow, D. Karaiskaj, X. Dai, T. Zhang, C. Carlsson, K. R. Hagen, R. Jimenez, and S. T. Cundiff, Rev. Sci. Instrum. **80**, 073108 (2009).
[10] P. Dey, J. Paul, J. Bylsma, S. Deminico, and D. Karaiskaj, Rev. Sci. Instrum. **84**, 023107 (2013).
[11] M. Koch, J. Feldmann, G. von Plessen, E. O. Göbel, P. Thomas, and K. Köhler, Phys. Rev. Lett. **69**, 3631 (1992).
[12] D. Karaiskaj, A. D. Bristow, L. Yang, X. Dai, R. P. Mirin, S. Mukamel, and S. T. Cundiff, Phys. Rev. Lett. **104**, 117401 (2010).
[13] C. N. Borca, T. Zhang, X. Li, and S. T. Cundiff, Chem. Phys. Lett. **416**, 311 (2005).
[14] Tianhao Zhang, Irina Kuznetsova, Torsten Meier, Xiaoqin Li, Richard P. Mirin, Peter Thomas, and Steven T. Cundiff, Proc. Natl. Acad. Sci. U.S.A. **104**, 14227 (2007).
[15] E. Runge and E. K. U. Gross, Phys. Rev. Lett. **52**, 997 (1984).
[16] D. S. Chemla and J. Shah, Nature (London) **411**, 549 (2001).
[17] S. W. Koch, M. Kira, G. Khitrova, and H. M. Gibbs, Nat. Mater. **5**, 523 (2006).
[18] R. B. Laughlin, Phys. Rev. B **23**, 5632 (1981).
[19] M. Z. Hasan and C. L. Kane, Rev. Mod. Phys. **82**, 3045 (2010).
[20] A. Pinczuk, J. P. Valladares, D. Heiman, A. C. Gossard, J. H. English, C. W. Tu, L. Pfeiffer, and K. West, Phys. Rev. Lett. **61**, 2701 (1988).
[21] A. Pinczuk, S. Schmitt-Rink, G. Danan, J. P. Valladares, L. N. Pfeiffer, and K. W. West, Phys. Rev. Lett. **63**, 1633 (1989).
[22] A. Pinczuk, B. S. Dennis, D. Heiman, C. Kallin, L. Brey, C. Tejedor, S. Schmitt-Rink, L. N. Pfeiffer, and K. W. West, Phys. Rev. Lett. **68**, 3623 (1992).
[23] A. Pinczuk, B. S. Dennis, L. N. Pfeiffer, and K. West, Phys. Rev. Lett. **70**, 3983 (1993).
[24] D. Heiman, B. B. Goldberg, A. Pinczuk, C. W. Tu, A. C. Gossard, and J. H. English, Phys. Rev. Lett. **61**, 605 (1988).
[25] B. B. Goldberg, D. Heiman, A. Pinczuk, L. Pfeiffer, and K. West, Phys. Rev. Lett. **65**, 641 (1990).
[26] B. B. Goldberg, D. Heiman, and A. Pinczuk, Phys. Rev. Lett. **63**, 1102 (1989).
[27] M. A. Eriksson, A. Pinczuk, B. S. Dennis, S. H. Simon, L. N. Pfeiffer, and K. W. West, Phys. Rev. Lett. **82**, 2163 (1999).
[28] M. Kang, A. Pinczuk, B. S. Dennis, M. A. Eriksson, L. N. Pfeiffer, and K. W. West, Phys. Rev. Lett. **84**, 546 (2000).
[29] M. Kang, A. Pinczuk, B. S. Dennis, L. N. Pfeiffer, and K. W. West, Phys. Rev. Lett. **86**, 2637 (2001).
[30] C. F. Hirjibehedin, A. Pinczuk, B. S. Dennis, L. N. Pfeiffer, and K. W. West, Phys. Rev. Lett. **91**, 186802 (2003).
[31] I. Dujovne, A. Pinczuk, M. Kang, B. S. Dennis, L. N. Pfeiffer, and K. W. West, Phys. Rev. Lett. **90**, 036803 (2003).
[32] I. Dujovne, A. Pinczuk, M. Kang, B. S. Dennis, L. N. Pfeiffer, and K. W. West, Phys. Rev. Lett. **95**, 056808 (2005).
[33] Y. Gallais, T. H. Kirschenmann, I. Dujovne, C. F. Hirjibehedin, A. Pinczuk, B. S. Dennis, L. N. Pfeiffer, and K. W. West, Phys. Rev. Lett. **97**, 036804 (2006).
[34] J. G. Groshaus, I. Dujovne, Y. Gallais, C. F. Hirjibehedin, A. Pinczuk, Y.-W. Tan, H. Stormer, B. S. Dennis, L. N. Pfeiffer, and K. W. West, Phys. Rev. Lett. **100**, 046804 (2008).
[35] K. Leo, M. Wegener, J. Shah, D. S. Chemla, E. O. Göbel, T. C. Damen, S. Schmitt-Rink, and W. Schäfer, Phys. Rev. Lett. **65**, 1340 (1990).
[36] P. Kner, S. Bar-Ad, M. V. Marquezini, D. S. Chemla, R. Lövenich, and W. Schäfer, Phys. Rev. B **60**, 4731 (1999).
[37] P. Dey, J. Paul, J. Bylsma, S. Deminico, and D. Karaiskaj, Rev. Sci. Instrum. **84**, 023107 (2013).
[38] S. T. Cundiff, Opt. Express **16**, 4639 (2008).
[39] S. Mukamel, D. Abramavicius, L. Yang, W. Zhuang, I. V. Schweigert, and D. V. Voronine, Acc. Chem. Res. **42**, 553 (2009).
[40] M. Cho, *Two-Dimensional Optical Spectroscopy* (CRC Press, Boca Raton, FL, 2010), p. 378.
[41] P. Hamm and M. Zanni, *Concepts and Methods of 2D Infrared Spectroscopy* (Cambridge University Press, Cambridge, England, 2011), p. 286.
[42] K. W. Stone, K. Gundogdu, D. B. Turner, X. Li, S. T. Cundiff, and K. A. Nelson, Science **324**, 1169 (2009).
[43] D. Turner and K. Nelson, Nature (London) **466**, 1089 (2010).

[44] J. Bylsma, P. Dey, J. Paul, S. Hoogland, E. H. Sargent, J. M. Luther, M. C. Beard, and D. Karaiskaj, Phys. Rev. B **86**, 125322 (2012).
[45] P. Dey, J. Paul, N. Glikin, Z. D. Kovalyuk, Z. R. Kudrynskyi, A. H. Romero, and D. Karaiskaj, Phys. Rev. B **89**, 125128 (2014).
[46] P. Dey, J. Paul, G. Moody, C. E. Stevens, N. Glikin, Z. D. Kovalyuk, Z. R. Kudrynskyi, A. H. Romero, A. Cantarero, D. J. Hilton, and D. Karaiskaj, J. Chem. Phys. **142**, 212422 (2015).
[47] See Supplemental Material at http://link.aps.org/supplemental/10.1103/PhysRevLett.116.157401 for details related to the sample characterization. It also provides a detailed description of the optical Bloch equations and TDDFT theory.
[48] S. A. Brown, J. F. Young, Z. Wasilewski, and P. T. Coleridge, Phys. Rev. B **56**, 3937 (1997).
[49] J. Paul, P. Dey, T. Tokumoto, J. L. Reno, D. J. Hilton, and D. Karaiskaj, J. Chem. Phys. **141**, 134505 (2014).
[50] S. Mukamel, *Principles of Nonlinear Optical Spectroscopy* (Oxford University Press, New York, 1995).
[51] S. T. Cundiff, Phys. Rev. A **49**, 3114 (1994).
[52] T. Yajima and Y. Taira, J. Phys. Soc. Jpn. **47**, 1620 (1979).
[53] V. Turkowski and C. A. Ullrich, Phys. Rev. B **77**, 075204 (2008).
[54] V. Turkowski, A. Leonardo, and C. A. Ullrich, Phys. Rev. B **79**, 233201 (2009).
[55] V. Turkowski and M. N. Leuenberger, Phys. Rev. B **89**, 075309 (2014).
[56] A. Ramirez-Torres, V. Turkowski, and T. S. Rahman, Phys. Rev. B **90**, 085419 (2014).
[57] Y.-H. Kim and A. Görling, Phys. Rev. Lett. **89**, 096402 (2002).
[58] Y.-H. Kim and A. Görling, Phys. Rev. B **66**, 035114 (2002).
[59] G. Onida, L. Reining, and A. Rubio, Rev. Mod. Phys. **74**, 601 (2002).
[60] F. Rossi and T. Kuhn, Rev. Mod. Phys. **74**, 895 (2002).
[61] S. Baroni, A. D. Corso, S. de Gironcoli, P. Giannozzi, C. Cavazzoni, G. Ballabio, S. Scandolo, G. Chiarotti, P. Focher, A. Pasquarello, K. Laasonen, A. Trave, R. Car, N. Marzari, and A. Kokalj, http://www.pwscf.org/ (LDA XC potential, 111111 46 independent k-point mesh in the first Brillouin zone, energy cutoff 80 Ry).